Electrical Power and Energy Systems 174 (2026) 111517

Contents lists available at ScienceDirect

International Journal of Electrical Power and Energy Systems

journal homepage: www.elsevier.com/locate/ijepes

Configure-and-Bound: A fast heuristic for network topology reconfiguration ☆

Basel Morsy [a,b,*], Jochen Stiasny [b], Adolfo Anta [a], Jochen Cremer [b]

[a] Austrian Institute of Technology AIT GmbH, Giefinggasse 4, Vienna, 1210, Austria
[b] TU Delft, Mekelweg 5, Delft, 2628 CD, Netherlands

ARTICLE INFO

Keywords:
Congestion management
MILPs
Heuristics
Bus-bar splitting

ABSTRACT

Congestion management is a key challenge in power systems, and topology reconfiguration offers a promising solution. This paper introduces the Configure-and-Bound (C&B) algorithm to efficiently solve network topology reconfiguration (NTR) problems, focusing on substation switching and busbar splitting. By exploiting the locality effects of switching maneuvers, the C&B algorithm significantly reduces the computational time required to solve the NP-hard NTR problems, while achieving most of the cost savings achieved by exact methods. We explore the conditions under which the proposed C&B algorithm is most effective by classifying congestion into two broad classes; near congestion and far congestion. The locality condition and the foundation of the proposed algorithm generalize to a broader class of (power system) optimization problems. Case studies done on IEEE 39, 118, 240, 300, 500, 588, and 793 bus systems demonstrate that the proposed algorithm can reduce the computational runtime by up to 99% and achieve up to 99.9% similar costs relative to the global optimal solution.

1. Introduction

In 2023, EUR 4 billion has been spent on congestion management in the EU [1]. On 8 January 2021, the Continental Europe Synchronous Area was split into two areas [2]. While seemingly distinct, both events underscore the critical role of transmission network flexibility. In particular, topology reconfiguration emerges as a promising strategy to mitigate congestion costs and enhance system resilience against large-scale disturbances. As power systems are growing in complexity, the ability to adapt the transmission network has become increasingly valuable. Traditional grid operation assumes a fixed network topology, but in reality operators have some flexibility to reconfigure the grid by utilizing switching gear in substations. Network topology reconfiguration (NTR) entails the utilization of the available switching gear in substations to perform switching maneuvers through which transmission lines can be switched on/off (known in the literature as transmission switching) and substations could be split and reconfigured (known as substation switching). The role of NTR in power system operation is to reroute the power flows through changing the physical grid structure via switching.

Network topology reconfiguration has been investigated since the late 1980s [3–11]. NTR can lead to significant operational benefits, including but not limited to: alleviating congestion [12], overload reduction [13], reducing operating costs [14,15], enhancing system reliability [16,17], power system resilience [18], transient stability [19], voltage stability [20], short-circuit currents [21], enhancing renewable integration [22], and recently in hybrid AC/DC grids [23,24].

However, the complexity of solving the optimization models resulting from using NTR remains a prohibitive challenge that prevents NTR from being adopted in today's transmission system operation. In [25], the complexity of switching problems has been shown to be NP-hard requiring huge computational budget to solve. Transmission switching problem has gained most of the attention for addressing its complexity as seen in [26–34], unlike substation switching problem. However, it has been shown in [35] that any transmission switching solution can be obtained by solving a substations switching (i.e., substation reconfiguration and busbar splitting) problem, but the opposite is not true. A few heuristics have been developed to address the complexity of substation switching problems.

In [36] a partitioning-based method was introduced to identify substations to be switched. The method applies fuzzy C-means clustering algorithm to partition the network into congestion zones and apply splitting to boundary substations. In [37], an iterative heuristic method was proposed to solve direct current optimal power flow (DCOPF) with substation switching. The iterative procedure considers one switching action at a time. The non-convex nature of the substation switching problem makes the approach of applying a single switching action at a time prone to convergence toward local optima. In [38], a heuristic was

☆ This article is part of a Special issue entitled: 'Power network topology' published in International Journal of Electrical Power and Energy Systems.

* Corresponding author at: Austrian Institute of Technology AIT GmbH, Giefinggasse 4, Vienna, 1210, Austria.
E-mail address: basel.morsy@ait.ac.at (B. Morsy).

https://doi.org/10.1016/j.ijepes.2025.111517
Received 11 September 2025; Received in revised form 6 November 2025; Accepted 17 December 2025
Available online 6 January 2026

Nomenclature

Parameters

B_l	Susceptance of line l.
P_d	Demand at node d.
$\overline{P}_l$	Maximum capacity of line l.
C_g	Cost of dispatch for generator g.
C^{LS}	Cost of load shedding.
$M_l^{\mathcal{E}}, M_l^{\delta}$	Big-M constants for line l used in disjunctive constraints related with power-flow/phase-angle limits.

Sets and Indices

$\mathcal{N}$	Set of all buses.
$\mathcal{N}^{aux}$	Set of auxiliary buses in all substations.
$\mathcal{G}$	Set of all generators. Indexed by g.
$\mathcal{D}$	Set of all loads. Indexed by d.
$\mathcal{L}$	Set of original (non-auxiliary) lines. Indexed by l.
$\mathcal{E}^r$	Set of auxiliary reconfiguration (switchable) lines in all substations. Subscript i is used to refer to the subset in substation i.
$\mathcal{E}^c$	Set of auxiliary coupler (switchable) lines in all substations. Subscript i is used to refer to the subset in substation i.
f_l	Origin node index of line l.
t_l	Terminal node index of line l.

Variables

P_g	Output power of generator g.
P_l	Power flow in line l.
δ_i	Voltage phase angle of bus i.
z_l^r	Switching status of substation reconfiguration auxiliary line l.
z_l^c	Switching status of bus-bar coupler l.
P_d^{LS}	Load shedding at node d.

proposed to solve NTR incorporating alternating current optimal power flow (ACOPF) and N-1 constraints. The method in [38] suffers from the limited number of allowed switching actions. In [39] a heuristic method was introduced to solve a specific version of NTR designed to improve feasibility of a power network for a fixed generation dispatch. The proposed algorithm in the [39] is iterative and applies one switching action at each iteration which suffers from the drawbacks mentioned earlier. The previous works do not consider the special structure of the NTR problem (i.e., some binary variables are more entangled together than others in case of substation switching), nor do they investigate the local/global effects of switching maneuvers on the power grid. The previously mentioned heuristics are based on an algorithm known as *k-opt* [40]. The k-opt algorithm is an iterative algorithm that applies k changes to a given feasible solution per iteration to find a better solution. The k-opt heuristic has been applied extensively to combinatorial optimization problems. An improvement to the k-opt algorithm is the Lin-Kernighan (LK) algorithm that assumes a variable k [41]. The state-of-the-art heuristic in that context is the Lin-Kernighan-Helsgaun (LKH) algorithm which was first introduced in [42]. The LKH algorithm uses a variable k and employs a restriction on the candidate set at each iteration utilizing domain knowledge (i.e., in the context of the traveling salesman problem, where these algorithms where first introduced, the domain knowledge is based on minimum spanning trees).

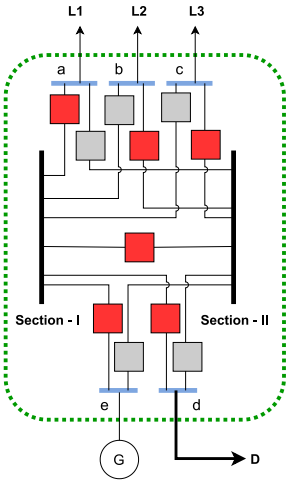

Fig. 1. Example of augmented network representation of a substation (enclosed by a dashed rectangle). switched on auxiliary line switched off auxiliary line auxiliary bus. L represents a transmission line, D for demand, and G for generator.

Paper contribution. This paper proposes a novel heuristic algorithm to address the complexity of network topology reconfiguration (NTR) problems arising in real-time or day-ahead operation planning. The paper investigates the locality effects of congestion and switching maneuvers on the grid and accordingly we classify congestion into two classes based on location — near congestion (when congested lines share a common node) and far congestion. The proposed algorithm leverages the locality effects of NTR. We show that the proposed algorithm can achieve most of the savings potential in a fraction of the required computational time for solving the problem exactly. We further identify the conditions under which the algorithm is most effective.

2. Preliminaries

2.1. Modeling substation switching

We model substation switching via Augmented Network Representation (ANR) [17]. Where each element connected to a substation (e.g. generator, load, transmission line, etc.) is assigned an auxiliary bus (illustrated in blue in Fig. 1). The two sections of the substation's bus-bar are connected through a bus-bar coupler. The coupler is modeled as a switchable auxiliary line (coupler line) and is used to model splitting/merging actions. Each auxiliary bus is connected to the two sections of the substation via switchable auxiliary lines (reconfiguration lines). A grid component can only be connected to one bus-bar section at any time. Auxiliary lines have zero impedance as in practice these switches have very small impedance values. Such small values introduce numerical instabilities and ill-conditioning for the solver. Auxiliary lines are also assumed to have high capacity (modeled here at least as high as all the capacities of connected grid components) to allow for power flow in any direction between the two bus-bar sections.

In this work, we consider linear physics of the grid based on the DCOPF approximation. We model substation switching with two sets of constraints for both substation reconfiguration and bus-bar splitting. Substation reconfiguration is the action of assigning grid components (connected to the substation in question) to bus-bar sections. Bus-bar splitting/merging is the action of switching off/on the bus-bar coupler. Substation reconfiguration constraints can be written as:

$$z_l^r \in \{0,1\}, \quad \forall l \in \mathcal{E}^r \tag{1a}$$

$$\sum_{l\in\mathcal{E}_i^r} z_l^r = 1, \quad \forall i \in \mathcal{N}^{aux} \tag{1b}$$

$$|\delta_{f_l} - \delta_{t_l}| \le (1 - z_l^r) M_l^{\delta}, \quad \forall l \in \mathcal{E}^r \tag{1c}$$

$$|P_l| \le z_l^r M_l^{\mathcal{E}}, \quad \forall l \in \mathcal{E}^r \tag{1d}$$

where constraint (1b) ensures that each auxiliary bus is connected to only one auxiliary line (mutual exclusivity) to avoid circular flows inside the substation. Constraint (1c) ensures that the phase difference between an auxiliary bus and a section is zero if the auxiliary bus is connected to that section, otherwise the upper bound of the phase difference is set to M_l^{δ} to ensure that the phase angles of the bus-bar sections do not deviate too far from each other. Constraint (1d) models the capacity of auxiliary lines, where if the auxiliary line is switched off, the capacity becomes zero, otherwise a sufficiently large upper bound for the power flow across an auxiliary line is set to $M_l^{\mathcal{E}}$.

Bus-bar splitting constraints are:

$$z_l^c \in \{0,1\}, \quad \forall l \in \mathcal{E}^c \tag{2a}$$

$$|\delta_{f_l} - \delta_{t_l}| \le (1 - z_l^c) M_l^{\delta}, \quad \forall l \in \mathcal{E}^c \tag{2b}$$

$$|P_l| \le z_l^c M_l^{\mathcal{E}}, \quad \forall l \in \mathcal{E}^c \tag{2c}$$

where constraint (2b) ensures that if the substation is not split, then the substation is regarded as a single electrical node with one phase angle, otherwise the two bus-bar sections of the substation have an upper bound for the phase angle difference. The constraint (2c) models the capacity of the bus-bar couplers.

2.2. MILP formulation

Model (1) is a mixed-integer linear program (MILP) formulation for optimal power flow (OPF) with network topology reconfiguration, where (3a) is the total cost of operation including the cost of load shedding. Constraints (3b) enforce the generators capacity limits. Constraint (3c) enforces nodal balance on all nodes. Constraint (3d) is the power flow physics constraint across a branch (e.g. transmission line) based on the DC approximation, while (3e) enforces the branch thermal capacities. Constraint (3f) limits the load shedding to be at most equal to the demand at each node.

Model 1. OPF-NTR

$$\min_{\boldsymbol{\delta},\boldsymbol{P},\boldsymbol{z^r},\boldsymbol{z^c},\boldsymbol{P^{LS}}} \quad \sum_{g\in\mathcal{G}} C_g P_g + \sum_{d\in D} C^{LS} P_d^{LS} \tag{3a}$$

$$\text{s.t.: } P_g^{min} \le P_g \le P_g^{max}, \quad \forall g \in \mathcal{G} \tag{3b}$$

$$\sum_{\forall g\in\mathcal{G}_i} P_g - \sum_{\forall d\in D_i} (P_d - P_d^{LS}) = \sum_{\forall l\in\mathcal{L}|f_l=i} P_l - \sum_{\forall l\in\mathcal{L}|t_l=i} P_l, \quad \forall i \in \mathcal{N} \tag{3c}$$

$$P_l = B_l(\delta_{f_l} - \delta_{t_l}), \quad \forall l \in \mathcal{L} \tag{3d}$$

$$-\overline{P}_l \le P_l \le \overline{P}_l, \quad \forall l \in \mathcal{L} \tag{3e}$$

$$0 \le P_d^{LS} \le P_d, \quad \forall d \in \mathcal{D} \tag{3f}$$

(1),(2) (3g)

3. Methodology

3.1. Exploiting structure

Theoretically, a substation can be split into two or more nodes, however, in practice splitting into two nodes is most relevant due to operational considerations (i.e., additional bus-bar sections are usually used for maintenance). The number of possible configurations upon splitting a substation with n_s elements into two nodes is 2^{n_s}. This large solution space (exponential in number of connections) is hard to handle efficiently by branch-and-bound algorithms. However, there is an underlying structure in this solution space that can be exploited. This solution space can be counted in a slightly different way using combinatorics.

Let S be a substation that can be split into two nodes S_a and S_b. Assume there are n_s elements connected to S (i.e., modeled via binary variables). The number of all possible combinations (i.e., the solution space $|S|$) can be written in the following compact formula:

$$|S| = 2^{n_s} = \sum_{k=0}^{n_s} \binom{n_s}{k} \tag{4}$$

This combinatorial expansion can be derived from counting the number configurations in each *configuration family*. We define a configuration family as:

Definition 1. A configuration family is a tuple that specifies how many elements are connected to each substation section.

$$\mathcal{F}_k^{n_s} := (k, n_s - k) \quad \forall k \in \{0, \dots, n_s\} \tag{5}$$

The size of each configuration family is given by:

$$|\mathcal{F}_k^{n_s}| = \binom{n_s}{k} \tag{6}$$

For example, a substation with 5 feeders can be split into two nodes rendered through the following vector $\mathbf{Z^r} = [0,1,0,1,1]$. This $\mathbf{Z^r}$ is one of the configurations that belong to the family $\mathcal{F}_3^5$. The family $\mathcal{F}_3^5$ has $\binom{5}{3} = 10$ possible configurations. Notice that $\mathbf{Z^r}$ is equivalent to $[1,0,1,0,0]$. In fact, all configurations in $\mathcal{F}_3^5$ are equivalent to all configurations in $\mathcal{F}_2^5$.

Each configuration family is essentially a possible way of reconfiguring the substation by connecting k elements to section S_a and $n_s - k$ elements to section S_b. We can notice here that there are redundant configuration families (e.g., assigning certain elements to one section or to the other yields equivalent configurations as shown earlier with $\mathbf{Z^r}$). Additionally, this solution space assumes that all configurations are allowed, which is not the case in practice. We can add some constraints to Model (1) that will reduce the solution space and capture more beneficial configurations if we know their corresponding configuration families as follows.

First, we define the set of substations that have a favorable configuration family $\mathcal{F}_k^{n_s}$ (for instance, identified via a heuristic) as

$$\mathcal{S}_k^{\text{fav}} := \{s \in \mathcal{N}^{\text{aux}} \mid s \text{ has family } \mathcal{F}_k^{n_s}\}.$$

Then, to enforce that the configuration family is respected for these substations, we impose the following constraint:

$$\sum_{l\in\mathcal{E}_{S_a}^r} z_l^r = k, \quad \forall s \in \mathcal{S}_k^{\text{fav}} \tag{7a}$$

$$\sum_{l\in\mathcal{E}_{S_b}^r} z_l^r = n_s - k, \quad \forall s \in \mathcal{S}_k^{\text{fav}} \tag{7b}$$

3.2. C&B algorithm

As previously discussed, each substation can be reconfigured into a finite number of distinct configuration families. The classical branch-and-bound (B&B) algorithm addresses such combinatorial problems by constructing a search tree in which each node represents a subproblem with one integer variable fixed. This reduces the problem to a linear program (LP), whose solution is then evaluated. If the solution is worse than the best known feasible (integer) solution (i.e., the incumbent), the branch is pruned. B&B is an exact method and guarantees global optimality by exhaustively exploring the feasible space while systematically eliminating suboptimal regions.

Table 1
Interpretation of the binary hyperparameters governing C&B algorithm.

Hyperparameter	Name & Scope	Interpretation of 0	Interpretation of 1
ρ_1	Self-relaxation. Used in the Oracle Problem (Algorithm 2).	Impose integrality on the focal substation.	Relax integrality.
ρ_2	Cross-relaxation. Used in the Oracle Problem.	Fix other substations to default topology.	Relax integrality for other substations.
ρ_3	Family fixing. Used in the Configuration Problem (Algorithm 3).	Configuration family of the focal substation has no impact	Fix configuration family of the focal substation as determined by the Oracle Problem
ρ_4	Multi-Oracle call. Used in the main C&B Algorithm (Algorithm 1)	Calls Oracle Problem once in the first iteration.	Calls Oracle Problem once in each iteration.
ρ_5	Revisit allowance. Used in the main C&B Algorithm	Visit each substation only once	Permit revisits after a full cycle for further refinement.

3.2.1. Intuition behind C&B algorithm

The intuition behind the C&B Algorithm is based on two hypotheses. First, the empirical observation that switching actions have a local effect. This hypothesis is supported in [43]. The locality property simply implies that one can solve the NTR model for one substation (a set of binary variables) at a time in an iterative fashion without losing too much degrees of freedom. Second, to solve for one substation at a time, we need to know the optimal order of substations (i.e., this is also a combinatorial problem of $n!$ possibilities for n substations). The NTR problem is usually non-convex even in its simplified mixed-integer linear program (MILP) form used in this work. Therefore, the proposed Configure-and-Bound (C&B) method introduces structure into the search by the natural grouping of substation reconfigurations. There are two objectives of C&B algorithm then; first, reduction of the solution space by optimizing one substation at a time. Second, optimal ordering of the substations to find better solutions.

3.2.2. Pseudo-code

The proposed Configure-and-Bound (C&B) algorithm (**Algorithm 1**) iteratively explores substation configurations by alternating between two subproblems: the *Oracle Problem* (**Algorithm 2**) and the *Configuration Problem* (**Algorithm 3**). The procedure maintains a set of visited substations $\mathcal{T}_{visited}$ and uses five binary hyperparameters $(\rho_1, \ldots, \rho_5)$ to regulate relaxations, primal cuts, and iteration control as detailed in Table 1.

Algorithm 1 (**C&B Procedure**) orchestrates both subproblems. It takes as inputs Model (1) after relaxation, the power grid model, and a combination of the five hyperparameters. It repeatedly invokes the oracle (**P1**) either once or at each iteration depending on ρ_4, selects the next substation to reconfigure, and updates the topology using (**P2**). The process terminates when all substations have been processed or when revisiting (controlled by ρ_5) yields no further improvement.

Algorithm 2 (**Oracle Problem**) ranks substations according to their potential for improvement. For each substation s, it solves a relaxed instance of the MILP model under conditions determined by ρ_1 (self-relaxation) and ρ_2 (cross-relaxation), producing an objective value ϕ and a configuration family $\mathcal{F}$. The resulting scores Φ^s and families $\mathcal{F}^s$ guide subsequent configuration updates.

Finally, **Algorithm 3** (**Configuration Problem**) performs a local optimization on the substation selected by the oracle. Given the chosen substation s^* and its configuration family f^*, it reconstructs the model, imposes integrality, and optionally fixes the configuration family depending on ρ_3. The resulting optimal objective ϕ and topology τ are then integrated into the global state $\mathcal{T}_{visited}$.

There are two constraints on the hyperparameters:

1. ρ_1 cannot be set to 1 while ρ_3 is also set to 1. This is because if we relax the binary variables of a substation in the oracle problem **P1** the configuration families found will not be integer and cannot be imposed on the configuration problem **P2**.
2. ρ_5 can only be set to 1 if ρ_4 is set to 1. This means that revisiting substations in the configuration problem **P2** is only possible if multiple oracle **P1** calls is allowed.

Table 2
Capacity multipliers for 39-bus system to induce congestion where congested lines do not share a common substation.

Line	Capacity multiplier
(2–30)	1.5
(16–17)	0.1
(13–14)	0.5

Table 3
Lines reduced to 0.3 of their capacities for different systems.

System	Reduced lines
118	52, 82, 23
240	130, 365, 435
300	85, 316, 337
500	135, 141, 248, 388, 451
588	52, 218, 420, 497, 567
793	51, 215, 420, 432, 685, 700

4. Results

In this section, we first investigate the applicability of NTR (when it is useful), and then investigate the applicability and scaling properties of the proposed C&B algorithm. We report the performance of the variant that achieved the best trade-off between solution quality and computational effort based on an extensive ablation study (see Appendix). The chosen variant has hyperparameters $\boldsymbol{\rho} = [1, 0, 0, 0, 0]$.

4.1. Experimental setup

We demonstrate the effectiveness of the proposed algorithm and compare it to solving the full NTR model directly using Gurobi. We use Julia language for modeling and calculations. The systems used can be found in the PGLib repository [44]. All experiments were conducted on a computer equipped with 32 GB of RAM and a CPU Intel core i7-1185G7.

The test cases are the 39-bus system to demonstrate the applicability of NTR and C&B, and the 118, 240, 300, 500, 588, and 793 bus systems to investigate the scaling properties of the proposed C&B algorithm.

Slight modifications to the test cases were made to induce congestions in different locations. The modifications were mainly multipliers applied to some transmission lines capacities. While the exact reduction of line capacities might not happen in reality, the congestion itself is the point of interest and it could happen due to many reasons (e.g. partial failure of circuits, etc.), but this is outside the scope of this work. In Table 2 the capacity multipliers are shown for the 39-bus system to induce congestion in two lines that do not share a common node. Similarly, in Table 3, the capacity multiplier used for each specified line is 0.3. The line index is based on its index in the PGLib ".m" files [44]. The nodes selected for splitting in all the experiments presented in this paper are the nodes peripheral to the congested lines, which is a common practice. In Fig. 2, the modified and original IEEE 39-bus systems are shown to indicate far and near congestions respectively.

(a) (b)

Fig. 2. 39-bus system: (a) congested lines share a common substation (original), and (b) congested lines do not share a common substation (modified). Red lines are congested lines, arrows point to the direction of power flow based on DCOPF.

Algorithm 1 Generic C&B Procedure

Input: Relaxed model $\mathcal{M}^{base}$, power grid $\mathcal{G}$, hyperparameters $(\rho_1, \rho_2, \rho_3, \rho_4, \rho_5)$
Output: Optimal objective ϕ_i, final topology $\mathcal{T}_{visited}$

Initialize *terminate* ← false, $\phi_i, \phi_{i-1} \leftarrow \emptyset$, $\mathcal{T}_{visited} \leftarrow \emptyset$
Initialize $\tau_i, \tau_{i-1}, v \leftarrow \emptyset$, $i \leftarrow 0$
while not *terminate* **do**
  $i \leftarrow i + 1$
  if $\rho_4 = 1$ **or** $i = 1$ **then**
    $(\boldsymbol{\Phi}^s, \mathcal{F}^s) \leftarrow$ **P1**$(\mathcal{G}, \mathcal{M}^{base}, \rho_1, \rho_2, \mathcal{T}_{visited})$ ▷ Oracle problem.
  end if
  if $\rho_5 = 1$ **and** KEYS$(\mathcal{T}_{visited})$ = SUBSTATIONS$(\mathcal{G})$ **then**
    $\boldsymbol{\Phi}^s \leftarrow \boldsymbol{\Phi}^s \setminus \{v\}$
  else
    $\boldsymbol{\Phi}^s \leftarrow \boldsymbol{\Phi}^s \setminus$ keys$(\mathcal{T}_{visited})$
  end if
  $s^* \leftarrow \arg\min \boldsymbol{\Phi}^s$
  $f^* \leftarrow \mathcal{F}^s_{s^*}$
  $(\phi_i, \tau_i) \leftarrow$ **P2**$(\mathcal{G}, \mathcal{M}^{base}, s^*, \rho_3, f^*, \mathcal{T}_{visited})$ ▷ Configuration problem
  $v \leftarrow s^*$
  if $\rho_5 = 1$ **then**
    if KEYS$(\mathcal{T}_{visited})$ = SUBSTATIONS$(\mathcal{G})$ **and** $\phi_i \geq \phi_{i-1}$ **then**
      terminate ← true
      $\phi_i \leftarrow \phi_{i-1}$, $\tau_i \leftarrow \tau_{i-1}$
    else
      $\mathcal{T}_{visited} \leftarrow \mathcal{T}_{visited} \cup \tau_i$
      $\phi_{i-1} \leftarrow \phi_i$, $\tau_{i-1} \leftarrow \tau_i$
    end if
  else
    $\mathcal{T}_{visited} \leftarrow \mathcal{T}_{visited} \cup \tau_i$
    if KEYS$(\mathcal{T}_{visited})$ = SUBSTATIONS$(\mathcal{G})$ **then**
      terminate ← true
    end if
  end if
end while
return $\phi_i, \mathcal{T}_{visited}$

Algorithm 2 Oracle Problem P1

Input: Power grid $\mathcal{G}$, relaxed model $\mathcal{M}^{base}$, hyperparameters (ρ_1, ρ_2), visited topologies $\mathcal{T}_{visited}$
Output: Objective scores $\boldsymbol{\Phi}^s$, families $\mathcal{F}^s$

Initialize $\boldsymbol{\Phi}^s$, $\mathcal{F}^s$ as empty dictionaries
for all $s \in$ Substations$(\mathcal{G})$ **in parallel do**
  $\mathcal{M} \leftarrow$ COPYMODEL$(\mathcal{M}^{base})$
  if $\rho_1 = 0$ **then**
    IMPOSEINTEGRALITY$(\mathcal{G}, \mathcal{M}, s)$
  end if
  if $\rho_2 = 1$ **then**
    $\mathcal{T}^{default} \leftarrow$ empty dictionary
  else
    $\mathcal{T}^{default} \leftarrow$ GRIDDEFAULTTOPOLOGY$(\mathcal{G}, \text{exclude} = \{s\})$
  end if
  Update $\mathcal{T}^{default}$ with entries from $\mathcal{T}_{visited}$
  FIXOTHERELEMENTS$(\mathcal{M}, \mathcal{T}^{default})$
  OPTIMIZE$(\mathcal{M})$
  if $\mathcal{M}$ has feasible solution **then**
    $\phi \leftarrow$ OBJECTIVEVALUE$(\mathcal{M})$
    $\mathcal{T} \leftarrow$ EXTRACTTOPOLOGY$(\mathcal{G}, \mathcal{M}, s)$
  else
    $\phi \leftarrow \infty$, $\mathcal{T} \leftarrow$ DEFAULTTOPOLOGY$(\mathcal{G}, s)$
  end if
  $\mathcal{F} \leftarrow$ EXTRACTFAMILY$(\mathcal{T})$
  $\boldsymbol{\Phi}^s[s] \leftarrow \phi$
  $\mathcal{F}^s[s] \leftarrow \mathcal{F}$
end for
return $\boldsymbol{\Phi}^s$, $\mathcal{F}^s$

4.2. Effectiveness of NTR

The following case study demonstrates the effectiveness of NTR. The experiment is conducted on the two variants of the IEEE 39-bus system presented in Fig. 2, the original system and the modified system. We vary the loading level from 90% to 120% of the nominal load. The loading level is a scaler multiplied by all the loads in the test case. We show the operating cost for both the DCOPF case (no switching) and solving the full NTR model case. We call the case where congested lines share a common bus "near congestion" (original system), while when the congested lines do not share a common bus, we call this case "far congestion" (modified system).

Fig. 3 shows the operating cost of NTR compared to DCOPF in the near congestion case. In Fig. 4, we show the operating costs for NTR and DCOPF in the far congestion case. Notably, the benefits of NTR in the far congestion case are more prominent. The loading level at which NTR starts to bring value to the operation (by reducing operating cost) is 110% for the near congestion case and 105% for the far congestion case. This case study signifies that NTR can bring more benefit to cases where congested lines are far away (at least not sharing a common bus).

In both cases presented in Figs. 3 and 4, we observe that as the loading level increases, the cost savings increase as well. This observation points out the fact that as the system becomes more stressed, NTR offers extra degrees of freedom to reroute the power flows.

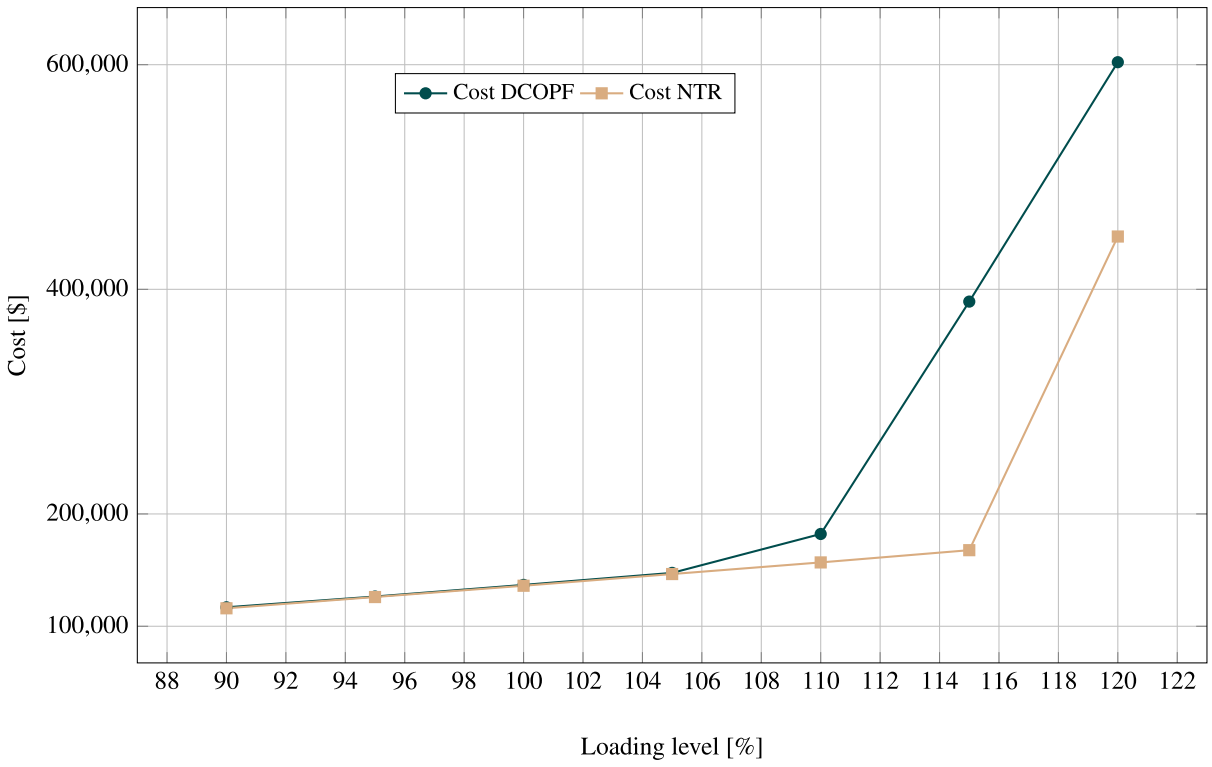

Fig. 3. Cost vs. Loading level for near congestion IEEE-39 bus system.

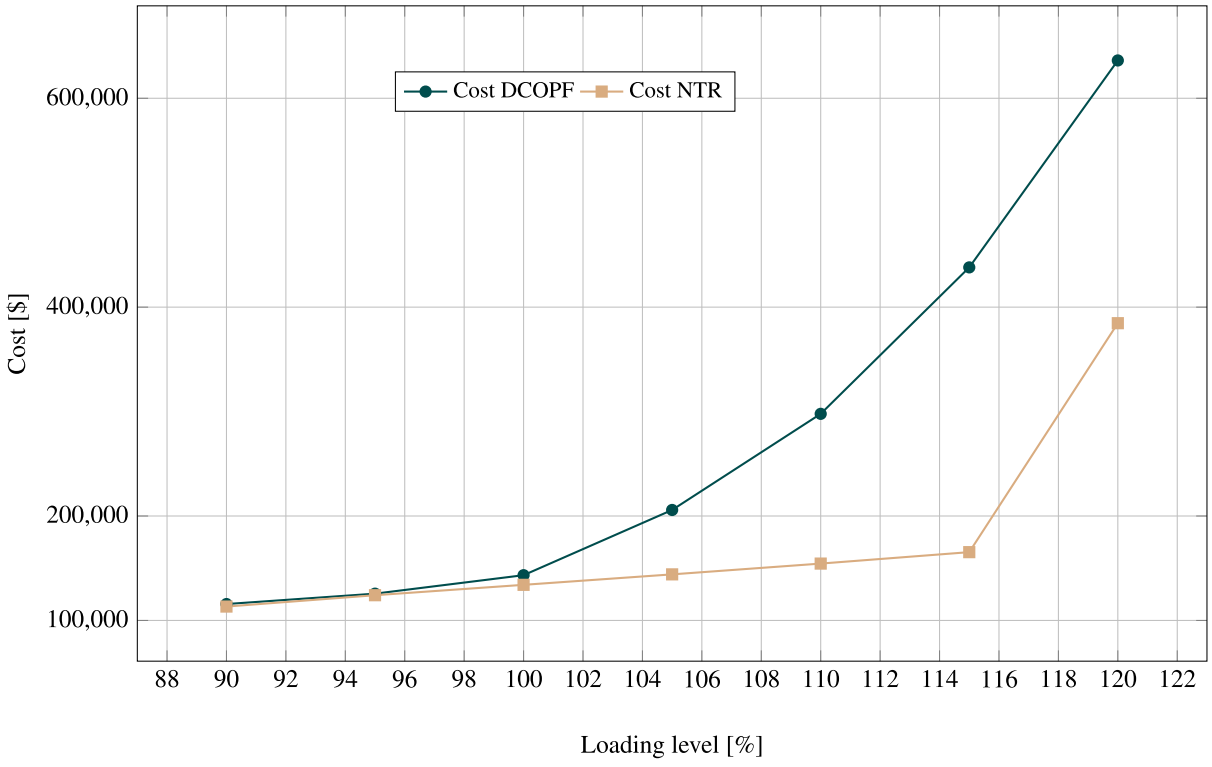

Fig. 4. Cost vs. Loading level for far congestion IEEE-39 bus system.

Fig. 5 shows the computational time taken to solve the full NTR model for the 39-bus system in both near and far congestion conditions. It is evident that the far congestion case requires more time to solve, hence more computationally expensive and needs more efficient algorithms to solve.

4.3. Results of the proposed C&B algorithm

In this case study, we show the effectiveness of the proposed C&B algorithm variants with systems of realistic sizes. We tested the algorithm with the IEEE 118, 240, 300, 500, 588, and 793 bus systems. We

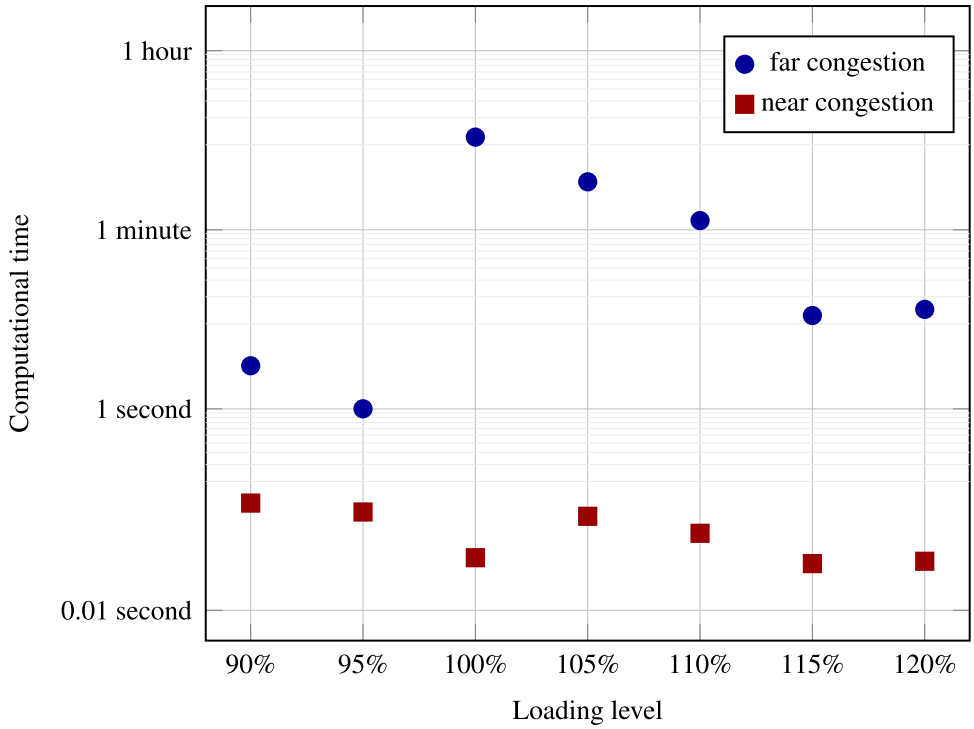

Fig. 5. Semi-log scale plot depicting computational time of NTR for near and far congestion cases.

Algorithm 3 Configuration Problem P2

Input: Power grid $\mathcal{G}$, relaxed model $\mathcal{M}^{base}$, current substation s^*, hyperparemeter ρ_3, configuration family of current substation f^*, topologies of previously visited substations $\mathcal{T}_{visited}$

Output: Objective value ϕ, optimal topology found for current substation τ

Initialize $\phi \leftarrow \infty$, $\tau \leftarrow \emptyset$
$\mathcal{M} \leftarrow$ CopyModel($\mathcal{M}^{base}$)
ImposeIntegrality($\mathcal{G}, \mathcal{M}, s^*$)
$\mathcal{T}^{default} \leftarrow$ GridDefaultTopology($\mathcal{G}$, exclude = $\{s\}$)
Update $\mathcal{T}^{default}$ with entries from $\mathcal{T}_{visited}$
FixOtherElements($\mathcal{M}, \mathcal{T}^{default}$)
if $\rho_3 = 1$ **then**
    ImposeFamily($\mathcal{G}, \mathcal{M}, s^*, f^*$)
end if
Optimize($\mathcal{M}$)
if $\mathcal{M}$ has feasible solution **then**
    $\phi \leftarrow$ ObjectiveValue($\mathcal{M}$)
    $\tau \leftarrow$ ExtractTopology($\mathcal{G}, \mathcal{M}, s$)
else
    $\phi \leftarrow \infty$, $\tau \leftarrow$ DefaultTopology($\mathcal{G}, s$)
end if
return ϕ, τ

used the iterative switching method found in the literature (i.e., known as the *1-opt* approach) as a heuristic baseline, in addition to solving the full NTR problem using Gurobi. Our procedure of applying capacity multiplier to some of the transmission lines induced congestion at different locations while ensuring that no two congested lines share a common node. Fig. 6 shows the scaling properties of the proposed C&B algorithm. The figure is a log–log scaled plot where the x-axis is the required computational time as a percentage of the computational time for solving the full NTR model. The y-axis is the ratio of the savings achieved by each algorithm to the savings achieved by solving the full NTR problem. The computational time limit for the full NTR model is set to 500 s, while no time limit is set for other methods. Most of the savings potential offered by topology reconfiguration is captured via the C&B algorithm (at least 70% in the studies presented), and most of the computational time requirement is also eliminated (at least 72%). The 1-opt heuristic, in the case of the 118-bus system required almost 50% of the computational time for solving the full NTR model. Table 4 shows the absolute numbers of objective values and computational times for all methods across all systems. In 5 out of the 6 case studies, the proposed C&B was able to find a solution in less time than the 1-opt algorithm, where in 3 of these 5 cases, the objective value found by C&B was better than that found by 1-opt. Fig. 7 shows that the 1-opt heuristic resorts to transmission switching more than the C&B. While in some problems transmission switching could be sufficient, it has been shown in [17] that in other cases a system could be N-1 vulnerable if corrective busbar splitting is not employed.

5. Discussion

The case studies presented in this paper show that there is a distinction between far congestion and near congestion. In the example presented (IEEE 39-bus case) to study the difference between the two cases, we observed two interesting insights. First, near congestion case was much less computationally expensive than the far congestion case, indicating that near congestion cases could be easier to solve. We reason this out to the tight coupling between the integer variables in the near congestion case. This tight coupling can lead to early pruning of branches in the branch-and-bound tree, leaving only a few feasible solutions. The second insight is that cost savings in near congestion case are generally less than cost savings in far congestion case. This confirms that NTR is more constrained (we lose some degrees of freedom) in the near congestion case than in the far congestion case. This insight also indicates the effect of switching is local, as this tight coupling of binary variables happen only in near congestion case.

Case studies on benchmarking the C&B algorithm against the full NTR model and the 1-opt heuristic (commonly used in the literature under different names) show that the proposed C&B algorithm excels at finding near-optimal solutions in fraction of the time needed by solving

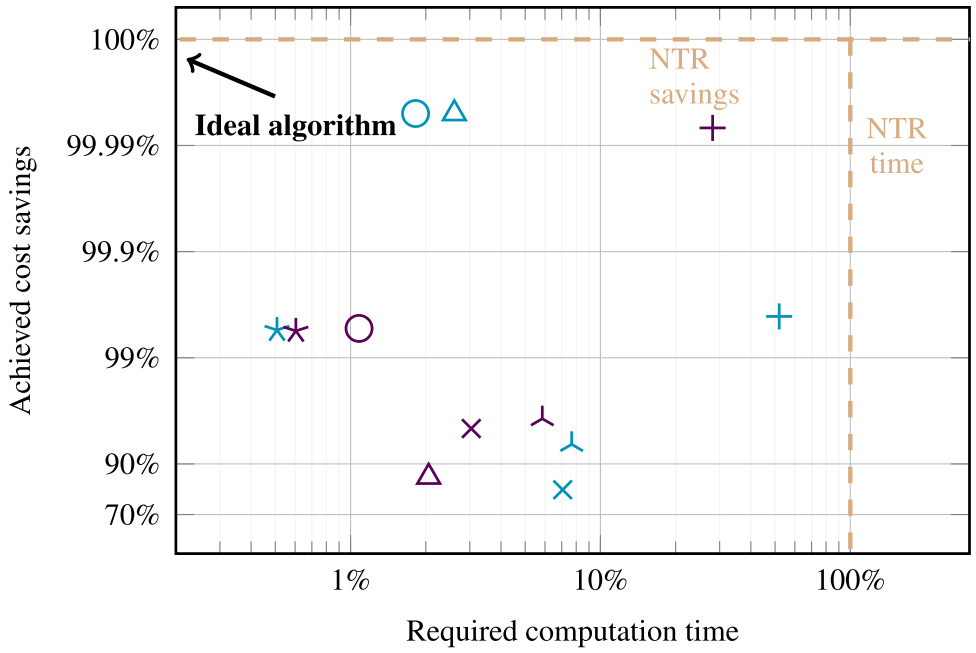

Fig. 6. Log–log scale plot of Cost savings vs. Computational time for different systems. Marker symbols indicate system size: + 118-bus, × 240-bus, ✱ 300-bus, ○ 500-bus, △ 588-bus, ⅄ 793-bus. Marker colors indicate method: ● 1-opt, ● GCnB-10000.

Table 4
Simulation results in absolute numbers.

System size	DCOPF		NTR		GCnB-10000		1-opt	
	Cost [$]	Time [s]	Cost [$]	Time [s]	Cost [$]	Time [s]	Cost [$]	Time [s]
118 (✱)	125,291.64	1.33	93,026.73	9.96	93,028.93	2.80	93,158.33	5.17
240 (○)	3.27×10^6	0.03	3.22×10^6	500.05	3.22×10^6	15.21	3.23×10^6	35.32
300 (⅄)	523,536.41	0.03	515,464.59	500.03	515,509.71	3.02	515,508.86	2.54
500 (×)	422,131.58	0.09	276,558.85	500.05	277,328.81	5.41	276,565.24	9.11
588 (△)	211,753.37	0.06	210,330.42	500.04	210,519.47	10.27	210,330.43	13.01
793 (+)	21,468.53	0.07	16,743.80	500.15	16,921.12	29.28	17,052.95	38.38

the full NTR model. We also observe that the proposed C&B algorithm dominates the 1-opt algorithm in finding substation switching solutions and not biased to finding only transmission switching solutions as is the case with the 1-opt algorithm. The computational time of the C&B algorithm is minimal, which shows the potential to use it for real-time or near-real-time switching maneuvers in realistic power grids where solving the full NTR model falls short in complying with realistic time constraints.

The notion of near/far congestion is only qualitatively defined in this work based on a simple assumption; congested lines that share a common substation qualify for near congestion, otherwise we considered the case as a far congestion case. Future work should address quantifying distance between congested lines and study the variation in performance of the C&B algorithm (or any other algorithm for that matter) with respect to this distance. We propose investigating metrics like *electrical distance*, sensitivity of flow on a branch given change of flow in another branch (i.e., the extreme form of this is the line outage distribution factors *LODF*), *graph hops*, and other *proximity* measures from graph theory.

Finally, potential extension of the C&B algorithm in future work is in the following directions:

1. Leveraging the good performance of the C&B algorithm to be used as a warm start for finding good topologies and enhance that solution with exact methods.
2. C&B algorithm can be applied in the context of N-1 security constrained optimal power flow in conjunction with decomposition methods like Benders decomposition or column-and-constraint generation (CCG) as in [17] where the master problem is the bottleneck of computational time. Similarly with stochastic and robust optimization problems where usually a bi-level technique is applied similar to the CCG method.
3. Application of C&B in ACOPF context is also possible since the method mainly addresses the complexity of switching, so as long as the complexity of ACOPF is addressed through a convex relaxation (e.g. semi-definite program, or second-order cone program), then C&B can still be applied.
4. Application of C&B to multi-period OPF (e.g. unit commitment problem) in day-ahead planning via grouping of generators and time periods is also possible in a similar fashion to the grouping of a substation binary variables in a more tractable problem.

6. Conclusion

In this paper a novel algorithm was developed to tackle the complexity of network topology reconfiguration (NTR) by leveraging the locality effects of switching in power grids. We conclude that decoupling and decomposition methods that tackle the complexity of NTR problems should make use of the locality insight. The proposed C&B algorithm opens the doors for real world applications of NTR in

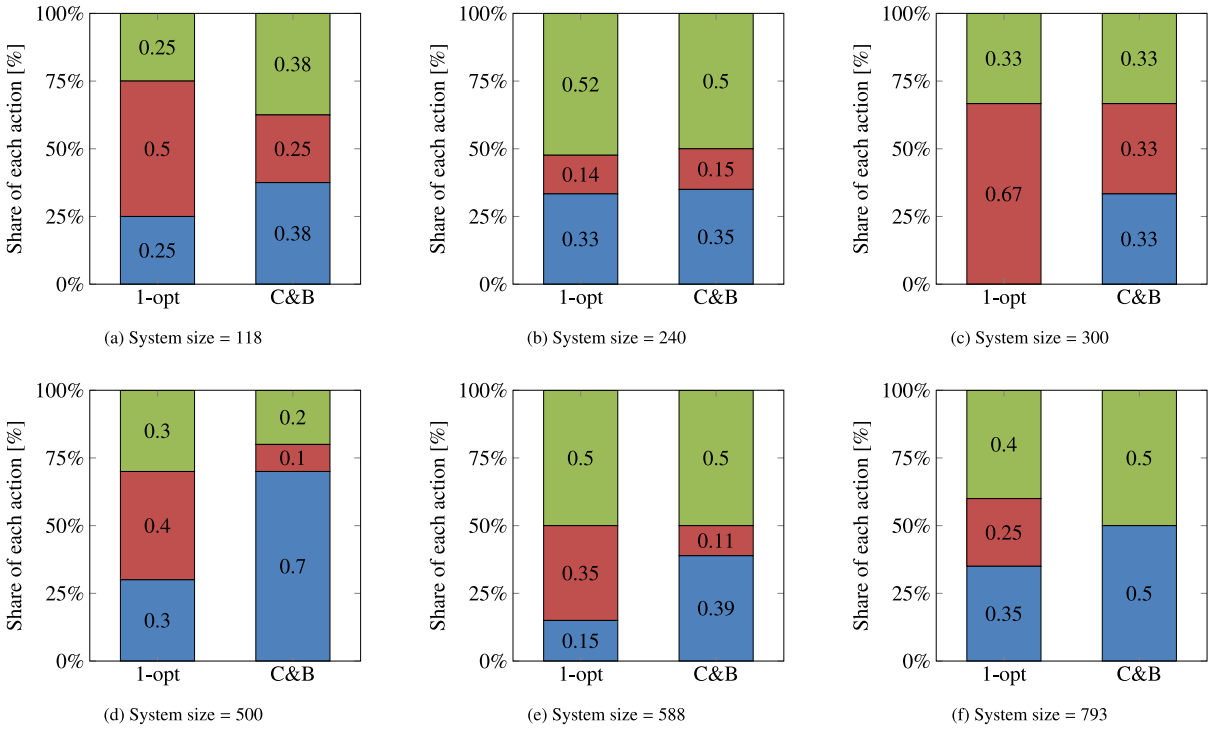

(a) System size = 118 (b) System size = 240 (c) System size = 300

(d) System size = 500 (e) System size = 588 (f) System size = 793

Fig. 7. Stacked bar plot showing the percentage of substations that underwent splitting, only transmission switching, or were not affected at all.

Table A.5
Simulation results. **Bold** entries denote minimum among heuristic methods, while underlined entries denote methods in the Pareto front.

Method	118		240		300		500		588		793	
	Cost [$]	Time [s]	Cost [$]	Time [s]	Cost [$]	Time [s]	Cost [$]	Time [s]	Cost [$]	Time [s]	Cost [$]	Time [s]
DCOPF	125,291.64	1.33	3.27×10^6	0.03	523,536.41	0.03	422,131.58	0.09	211,753.37	0.06	21,468.53	0.07
NTR	93,026.73	9.96	3.22×10^6	500.05	515,464.59	500.03	276,558.85	500.05	210,330.42	500.04	16,743.80	500.15
C&B-00000	93,069.78	7.68	3.22×10^6	20.43	515,529.11	3.60	277,328.43	7.22	210,572.72	14.09	16,916.52	**27.53**
C&B-00010	93,030.19	7.40	3.22×10^6	153.44	515,485.71	14.51	276,609.28	27.86	210,519.47	111.29	16,831.85	229.98
C&B-00100	93,094.43	2.96	3.22×10^6	19.88	515,514.96	7.21	277,368.32	7.67	210,572.68	12.16	16,981.98	28.90
C&B-00110	93,029.24	9.13	3.22×10^6	150.69	515,501.48	13.94	276,608.00	29.64	210,519.47	110.74	16,829.37	240.82
C&B-01000	93,057.95	2.80	3.23×10^6	18.18	515,534.71	3.66	276,817.38	8.61	210,826.84	13.98	16,971.66	37.08
C&B-01010	93,057.95	7.09	3.23×10^6	188.60	515,548.35	20.03	276,859.52	26.67	210,762.90	129.16	16,964.71	347.97
C&B-01100	93,030.22	2.19	3.23×10^6	18.38	515,522.96	3.47	276,681.82	5.53	210,763.22	12.40	17,085.12	41.89
C&B-01110	93,027.86	7.11	3.23×10^6	184.99	515,517.56	19.65	276,612.77	26.73	210,592.88	133.39	16,937.81	350.62
C&B-10000	93,028.93	2.80	3.22×10^6	**15.21**	515,509.71	3.02	277,328.81	**5.41**	210,519.47	10.27	16,921.12	29.28
C&B-10010	93,159.88	9.20	3.22×10^6	126.47	515,494.40	10.24	276,618.17	22.15	210,371.47	100.17	16,851.63	243.05
C&B-11000	93,057.95	**1.84**	3.23×10^6	15.79	515,540.61	2.55	276,638.35	6.41	210,904.19	**10.26**	17,175.28	32.14
C&B-11010	93,057.95	5.93	3.23×10^6	130.79	515,540.61	11.90	276,638.35	23.56	210,904.19	99.13	17,175.28	247.55
C&B-00011	93,030.19	7.89	3.22×10^6	170.59	515,485.71	15.49	276,609.28	32.88	210,519.47	121.83	16,831.85	336.71
C&B-00111	93,029.24	10.05	3.22×10^6	164.21	515,501.48	16.37	276,608.00	31.57	210,519.47	118.67	16,829.37	327.82
C&B-01011	93,057.95	7.56	3.23×10^6	195.99	515,548.35	19.41	276,859.52	29.92	210,762.90	139.47	16,964.71	408.35
C&B-01111	93,027.86	9.42	3.23×10^6	193.74	515,517.56	18.10	276,612.77	28.78	210,592.88	144.94	16,937.81	383.57
C&B-10011	93,159.88	8.17	3.22×10^6	129.14	515,494.40	12.91	276,618.17	28.16	210,371.47	100.67	16,851.63	296.11
C&B-11011	93,057.95	9.14	3.23×10^6	142.07	515,540.61	14.05	276,638.35	23.54	210,904.19	111.49	17,175.28	297.40
1-opt	93,158.33	5.17	3.23×10^6	35.32	515,508.86	**2.54**	276,565.24	9.11	210,330.43	13.01	17,052.95	38.38
2-opt	**93,026.73**	5.68	3.22×10^6	98.46	515,485.19	3.81	276,565.23	13.21	**210,330.42**	16.99	16,989.88	64.81
3-opt	**93,026.73**	9.42	**3.22×10^6**	333.91	**515,468.49**	5.82	**276,558.85**	21.37	**210,330.42**	21.79	**16,823.22**	201.97

transmission networks, where congested lines usually do not share a common bus. The results shown in this paper indicate that C&B can achieve most of the benefit associated with NTR in a fraction of the required computational time to solve the actual full model.

CRediT authorship contribution statement

Basel Morsy: Writing – original draft, Visualization, Validation, Software, Methodology, Investigation, Formal analysis, Conceptualization. **Jochen Stiasny:** Writing – review & editing, Visualization, Supervision. **Adolfo Anta:** Writing – review & editing, Supervision, Formal analysis, Conceptualization. **Jochen Cremer:** Writing – review & editing, Supervision, Conceptualization.

Declaration of competing interest

The authors declare that they have no known competing financial interests or personal relationships that could have appeared to influence the work reported in this paper.

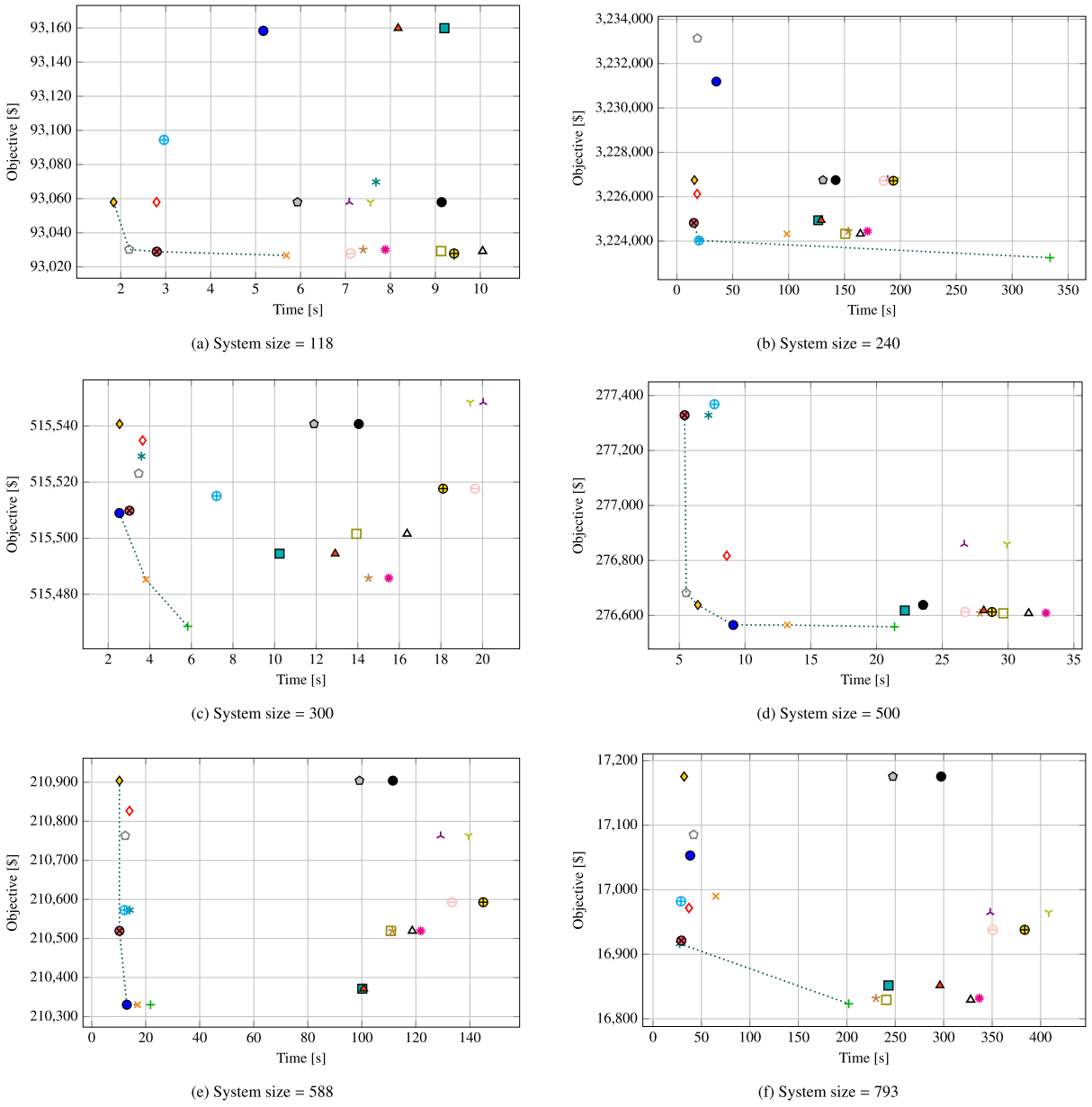

(a) System size = 118

(b) System size = 240

(c) System size = 300

(d) System size = 500

(e) System size = 588

(f) System size = 793

Fig. A.8. Pareto comparison of all methods. Markers denote methods as follows: ● 1-opt, × 2-opt, + 3-opt, ✱ C&B-00000, ✱ C&B-00010, ✱ C&B-00011, ⊕ C&B-00100, □ C&B-00110, ▲ C&B-00111, ◇ C&B-01000, ⅄ C&B-01010, ⅄ C&B-01011, ⬠ C&B-01100, ⊖ C&B-01110, ⊕ C&B-01111, ⊗ C&B-10000, ■ C&B-10010, ▲ C&B-10011, ◆ C&B-11000, ⬟ C&B-11010, ● C&B-11011.

Appendix. Ablation study

The *Configure-and-Bound* (C&B) heuristic is governed by five binary hyperparameters $(\rho_1, \ldots, \rho_5)$ controlling integrality, coupling, family fixing, multi-Oracle call execution, and revisits. In this appendix we present an ablation study showing the characteristics of each variant of the *Generic Configure-and-Bound* algorithm. Each variant of the algorithm will be denoted "C&B-" followed by a bit string of representing the values of the binary hyperparameters. We also added two more heuristic baselines, 2-opt and 3-opt.

Table A.5 shows the absolute numbers for objective values and runtimes of all methods.

Fig. A.8 shows the Pareto set (front) of methods for the test cases of different system sizes. We observe that as the k in k-opt methods increases, better objective values are achieved but at the expense of computational burden.

Finally, Fig. A.9 shows the frequency of appearance in the Pareto fronts for each C&B variant. C&B-10000 appears the most in the Pareto fronts, therefore it was chosen as the proposed C&B variant.

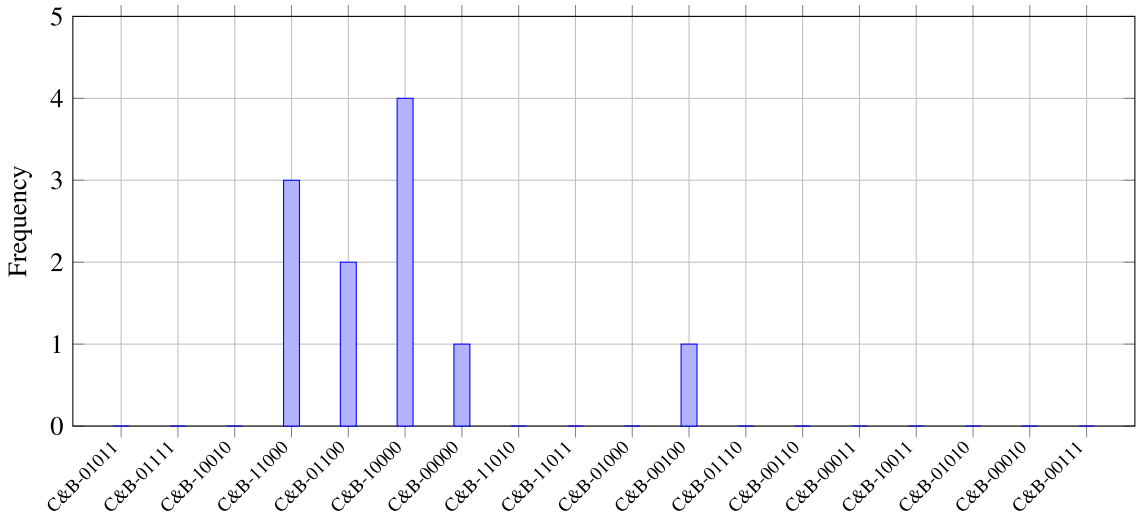

Fig. A.9. Bar plot of method frequency of appearance in Pareto fronts of each of the C&B variants.

References

[1] Agency for the Cooperation of Energy Regulators (ACER). ACER Market Monitoring Report 2024: Cross-zonal Electricity Trade Capacities. 2024, URL https://www.acer.europa.eu/monitoring/MMR/crosszonal_electricity_trade_capacities_2024, Accessed: [December 2024].

[2] ENTSO-E. Interim report on the continental Europe separation on 8 January 2021. Tech. rep., European Network of Transmission System Operators for Electricity; 2021, URL https://eepublicdownloads.azureedge.net/clean-documents/Publications/Position%20papers%20and%20reports/entso-e_CESysSep_interim_report_210225.pdf, [Accessed 16 April 2025].

[3] Koglin HJ, Müller H. Corrective switching: a new dimension in optimal load flow. Int J Electr Power Energy Syst 1982;4(2):142–9. http://dx.doi.org/10.1016/0142-0615(82)90041-2, URL https://www.sciencedirect.com/science/article/pii/0142061582900412.

[4] Rossier CA, Germond A, editors. Network topology optimization for power system security enhancement. 1983.

[5] Glavitsch H, Kronig H, Bacher R. Combined use of linear programming and load flow techniques in determining optimal switching sequences. In: Proceedings of the eighth power systems computation conference. Butterworth-Heinemann; 1984, p. 627–36. http://dx.doi.org/10.1016/B978-0-408-01468-7.50094-1, URL https://www.sciencedirect.com/science/article/pii/B9780408014687500941.

[6] Glavitsch H. Switching as means of control in the power system. Int J Electr Power Energy Syst 1985;7(2):92–100. http://dx.doi.org/10.1016/0142-0615(85)90014-6, URL https://www.sciencedirect.com/science/article/pii/0142061585900146.

[7] Koglin HJ, de Medeiros MF. Corrective switching approaching on-line application. IFAC Proc Vol 1985;18(7):203–7. http://dx.doi.org/10.1016/S1474-6670(17)60436-1, URL https://www.sciencedirect.com/science/article/pii/S1474667017604361.

[8] Bacher R, Glavitsch H. Network topology optimization with security constraints. IEEE Trans Power Syst 1986;1(4):103–11. http://dx.doi.org/10.1109/TPWRS.1986.4335024, Conference Name: IEEE Transactions on Power Systems.

[9] Mazi AA, Wollenberg BF, Hesse MH. Corrective control of power system flows by line and bus-bar switching. IEEE Trans Power Syst 1986;1(3):258–64. http://dx.doi.org/10.1109/TPWRS.1986.4334990, Conference Name: IEEE Transactions on Power Systems.

[10] Monticelli A, Pereira MVF, Granville S. Security-constrained optimal power flow with post-contingency corrective rescheduling. IEEE Trans Power Syst 1987;2(1):175–80. http://dx.doi.org/10.1109/TPWRS.1987.4335095, Conference Name: IEEE Transactions on Power Systems.

[11] Schnyder G, Glavitsch H. Integrated security control using an optimal power flow and switching concepts. IEEE Trans Power Syst 1988;3(2):782–90. http://dx.doi.org/10.1109/59.192935, Conference Name: IEEE Transactions on Power Systems.

[12] Nasrolahpour E, Ghasemi H, Khanabadi M. Optimal transmission congestion management by means of substation reconfiguration. In: 20th Iranian conference on electrical engineering. ICEE2012, 2012, p. 416–21. http://dx.doi.org/10.1109/IranianCEE.2012.6292394, ISSN: 2164-7054.

[13] Bakirtzis AG, Meliopoulos APS. Incorporation of switching operations in power system corrective control computations. IEEE Trans Power Syst 1987;2(3):669–75. http://dx.doi.org/10.1109/TPWRS.1987.4335192, Conference Name: IEEE Transactions on Power Systems.

[14] Fisher EB, O'Neill RP, Ferris MC. Optimal transmission switching. IEEE Trans Power Syst 2008;23(3):1346–55. http://dx.doi.org/10.1109/TPWRS.2008.922256, Conference Name: IEEE Transactions on Power Systems.

[15] Han J, Papavasiliou A. The impacts of transmission topology control on the European electricity network. IEEE Trans Power Syst 2016;31(1):496–507. http://dx.doi.org/10.1109/TPWRS.2015.2408439, Conference Name: IEEE Transactions on Power Systems.

[16] Babaeinejadsarookolaee S, Park B, Lesieutre B, DeMarco CL. Effective congestion management via network topology optimization based on node-breaker representations. In: 2022 north American power symposium. NAPS, 2022, p. 1–6. http://dx.doi.org/10.1109/NAPS56150.2022.10012243, ISSN: 2833-003X.

[17] Morsy B, Hinneck A, Pozo D, Bialek J. Security constrained OPF utilizing substation reconfiguration and busbar splitting. Electr Power Syst Res 2022;212:108507. http://dx.doi.org/10.1016/j.epsr.2022.108507, URL https://www.sciencedirect.com/science/article/pii/S0378779622006071.

[18] Trodden PA, Bukhsh WA, Grothey A, McKinnon KIM. MILP islanding of power networks by bus splitting. In: 2012 IEEE power and energy society general meeting. 2012, p. 1–8. http://dx.doi.org/10.1109/PESGM.2012.6345046, ISSN: 1944-9925.

[19] Owusu-Mireku R, Chiang H-D. A direct method for the transient stability analysis of transmission switching events. In: 2018 IEEE power & energy society general meeting. PESGM, 2018, p. 1–5. http://dx.doi.org/10.1109/PESGM.2018.8586242, ISSN: 1944-9933.

[20] Wang L, Chiang H-D. Bus-bar splitting for enhancing voltage stability under contingencies. Sustain Energy Grids Networks 2023;34:101010. http://dx.doi.org/10.1016/j.segan.2023.101010, URL https://www.sciencedirect.com/science/article/pii/S2352467723000188.

[21] Pati RS, Ghosh D. Busbar splitting approach for fault level management for system integrity protection scheme. In: 2020 first IEEE international conference on measurement, instrumentation, control and automation. ICMICA, 2020, p. 1–4. http://dx.doi.org/10.1109/ICMICA48462.2020.9242709.

[22] Mohseni-Bonab SM, Kamwa I, Rabiee A, Chung CY. Stochastic optimal transmission Switching: A novel approach to enhance power grid security margins through vulnerability mitigation under renewables uncertainties. Appl Energy 2022;305:117851. http://dx.doi.org/10.1016/j.apenergy.2021.117851, URL https://www.sciencedirect.com/science/article/pii/S0306261921011752.

[23] Bastianel G, Vanin M, Hertem DV, Ergun H. Optimal transmission switching and busbar splitting in hybrid AC/DC grids. 2024, arXiv:2412.00270, URL https://arxiv.org/abs/2412.00270.

[24] Morsy B, Deakin M, Anta A, Cremer J. Corrective soft bus-bar splitting for reliable operation of hybrid AC/DC grids. Int J Electr Power Energy Syst 2025;169:110792. http://dx.doi.org/10.1016/j.ijepes.2025.110792, URL https://www.sciencedirect.com/science/article/pii/S0142061525003400.

[25] Lehmann K, Grastien A, Hentenryck PV. The complexity of DC-switching problems. 2014, ArXiv, arXiv:1411.4369, URL https://api.semanticscholar.org/CorpusID:3175338.

[26] Ruiz PA, Foster JM, Rudkevich A, Caramanis MC. On fast transmission topology control heuristics. In: 2011 IEEE power and energy society general meeting. 2011, p. 1–8. http://dx.doi.org/10.1109/PES.2011.6039833, ISSN: 1944-9925.

[27] Ruiz PA, Foster JM, Rudkevich A, Caramanis MC. Tractable transmission topology control using sensitivity analysis. IEEE Trans Power Syst 2012;27(3):1550–9. http://dx.doi.org/10.1109/TPWRS.2012.2184777, Conference Name: IEEE Transactions on Power Systems.

[28] Goldis EA, Caramanis MC, Philbrick CR, Rudkevich AM, Ruiz PA. Security-constrained MIP formulation of topology control using loss-adjusted shift factors. In: 2014 47th hawaii international conference on system sciences. 2014, p. 2503–9. http://dx.doi.org/10.1109/HICSS.2014.313, ISSN: 1530-1605.

[29] Ruiz PA, Goldis EA, Rudkevich A, Caramanis MC, Philbrick CR, Foster JM. Security-constrained transmission topology control MILP formulation using sensitivity factors. IEEE Trans Power Syst 2016;1. http://dx.doi.org/10.1109/TPWRS.2016.2577689, URL http://ieeexplore.ieee.org/document/7486084/.

[30] Fuller JD, Ramasra R, Cha A. Fast heuristics for transmission-line switching. IEEE Trans Power Syst 2012;27(3):1377–86. http://dx.doi.org/10.1109/TPWRS.2012.2186155, Conference Name: IEEE Transactions on Power Systems.

[31] Liu C, Wang J, Ostrowski J. Heuristic prescreening switchable branches in optimal transmission switching. IEEE Trans Power Syst 2012;27(4):2289–90. http://dx.doi.org/10.1109/TPWRS.2012.2193489, Conference Name: IEEE Transactions on Power Systems.

[32] Wang S, Baillieul J. Power grid decomposition based on vertex cut sets and its applications to topology control and power trading. In: 2018 IEEE conference on decision and control. CDC, 2018, p. 4882–9. http://dx.doi.org/10.1109/CDC.2018.8619241, ISSN: 2576-2370.

[33] Fattahi S, Lavaei J, Atamtürk A. A bound strengthening method for optimal transmission switching in power systems. IEEE Trans Power Syst 2019;34(1):280–91. http://dx.doi.org/10.1109/TPWRS.2018.2867999, Conference Name: IEEE Transactions on Power Systems.

[34] Hinneck A, Pozo D. Optimal transmission switching: Improving exact algorithms by parallel incumbent solution generation. IEEE Trans Power Syst 2022;1–14. http://dx.doi.org/10.1109/TPWRS.2022.3199114, Conference Name: IEEE Transactions on Power Systems.

[35] Hinneck A, Morsy B, Pozo D, Bialek J. Optimal power flow with substation reconfiguration. In: 2021 IEEE madrid powerTech. 2021, p. 1–6. http://dx.doi.org/10.1109/PowerTech46648.2021.9494797.

[36] Heidarifar M, Ghasemi H. A network topology optimization model based on substation and node-breaker modeling. IEEE Trans Power Syst 2016;31(1):247–55. http://dx.doi.org/10.1109/TPWRS.2015.2399473.

[37] Babaeinejadsarookolaee S, Lesieutre B, DeMarco CL. Tractable iterative transmission topology control heuristics based on node-breaker modeling. In: 2021 56th international universities power engineering conference. UPEC, 2021, p. 1–6. http://dx.doi.org/10.1109/UPEC50034.2021.9548159.

[38] Heidarifar M, Andrianesis P, Ruiz P, Caramanis MC, Paschalidis IC. An optimal transmission line switching and bus splitting heuristic incorporating AC and N-1 contingency constraints. Int J Electr Power Energy Syst 2021;133:107278. http://dx.doi.org/10.1016/j.ijepes.2021.107278, URL https://www.sciencedirect.com/science/article/pii/S0142061521005172.

[39] Babaeinejadsarookolaee S, Park B, Lesieutre B, DeMarco CL. Transmission congestion management via node-breaker topology control. IEEE Syst J 2023;1–12. http://dx.doi.org/10.1109/JSYST.2023.3241805, Conference Name: IEEE Systems Journal.

[40] Lin S. Computer solutions of the traveling salesman problem. Bell Syst Tech J 1965;44(10):2245–69. http://dx.doi.org/10.1002/j.1538-7305.1965.tb04146.x.

[41] Lin S, Kernighan BW. An effective heuristic algorithm for the traveling-salesman problem. Oper Res 1973;21:498–516, URL https://api.semanticscholar.org/CorpusID:33245458.

[42] Helsgaun K. An effective implementation of the Lin-Kernighan traveling salesman heuristic. European J Oper Res 2000;126:106–30, URL https://api.semanticscholar.org/CorpusID:14802229.

[43] Barrows C, Blumsack S. Optimal transmission switching analysis and marginal switching results. In: 2011 IEEE power and energy society general meeting. 2011, p. 1–3. http://dx.doi.org/10.1109/PES.2011.6039669, ISSN: 1944-9925.

[44] Babaeinejadsarookolaee S, Birchfield A, Christie RD, Coffrin C, DeMarco C, Diao R, Ferris M, Fliscounakis S, Greene S, Huang R, Josz C, Korab R, Lesieutre B, Maeght J, Mak TWK, Molzahn DK, Overbye TJ, Panciatici P, Park B, Snodgrass J, Tbaileh A, Hentenryck PV, Zimmerman R. The power grid library for benchmarking AC optimal power flow algorithms. 2021, arXiv:1908.02788, URL https://arxiv.org/abs/1908.02788.